REPORT DOCUMENTATION PAGE

Form Approved OMB NO. 0704-0188

1. REPORT DATE (DD-MM-YYYY)	2. REPORT TYPE	3. DATES COVERED (From - To)
	Technical Report	-

4. TITLE AND SUBTITLE
Silica Entrapment of Biofilms in Membrane Bioreactors for Water Regeneration

5a. CONTRACT NUMBER
W911NF-09-1-0447

5b. GRANT NUMBER

5c. PROGRAM ELEMENT NUMBER
611102

6. AUTHORS
David Jaroch, Eric McLamore, Wen Zhang, Jin Shi, Jay Garland, M. Katherine Banks, D. Marshall Porterfield, Jenna L. Rickus

5d. PROJECT NUMBER

5e. TASK NUMBER

5f. WORK UNIT NUMBER

7. PERFORMING ORGANIZATION NAMES AND ADDRESSES
Indiana University - Purdue University Fort Wayn
Sponsored Programs Services
Young Hall, 302 Wood Street
West Lafayette, IN 47907 -2108

8. PERFORMING ORGANIZATION REPORT NUMBER

9. SPONSORING/MONITORING AGENCY NAME(S) AND ADDRESS(ES)
U.S. Army Research Office
P.O. Box 12211
Research Triangle Park, NC 27709-2211

10. SPONSOR/MONITOR'S ACRONYM(S)
ARO

11. SPONSOR/MONITOR'S REPORT NUMBER(S)
57197-EV.1

12. DISTRIBUTION AVAILIBILITY STATEMENT
Approved for public release; distribution is unlimited.

13. SUPPLEMENTARY NOTES
The views, opinions and/or findings contained in this report are those of the author(s) and should not contrued as an official Department of the Army position, policy or decision, unless so designated by other documentation.

14. ABSTRACT
Habitat systems for long-term resource recovery must be reliable, safe and highly efficient, while providing potable water, oxygen, and edible biomass. Water makes up a large portion of the daily mass input into habitat systems. Considerations for water recycling technologies include shelf life, resupply-return logistics, maintenance time, power requirements, and footprint. Water recovery via physicochemical processes is limited by resupply, which can be alleviated by incorporation of an autonomous bioregenerative core, utilizing innate metabolic activity of

15. SUBJECT TERMS
water regeneration, habitat systems, membrane-aerated bioreactor, silica membrane, biofilm, detachment

16. SECURITY CLASSIFICATION OF:			17. LIMITATION OF ABSTRACT	15. NUMBER OF PAGES	19a. NAME OF RESPONSIBLE PERSON
a. REPORT	b. ABSTRACT	c. THIS PAGE			Jenna Rickus
UU	UU	UU	UU		19b. TELEPHONE NUMBER: 765-494-1197

Report Title

Silica Entrapment of Biofilms in Membrane Bioreactors for Water Regeneration

ABSTRACT

Habitat systems for long-term resource recovery must be reliable, safe and highly efficient, while providing potable water, oxygen, and edible biomass. Water makes up a large portion of the daily mass input into habitat systems. Considerations for water recycling technologies include shelf life, resupply-return logistics, maintenance time, power requirements, and footprint. Water recovery via physicochemical processes is limited by resupply, which can be alleviated by incorporation of an autonomous bioregenerative core, utilizing innate metabolic activity of cells to recover useable water from various wastestreams. Major components of bioregenerative core systems include plant/crop production systems and microbial bioreactors.

One of the microbial bioreactor technologies currently under consideration for use within closed loop water recovery systems is the membrane-aerated bioreactor (MABR). Although many advancements have been made regarding the optimization of MABR biotechnologies, problems that persist include: slow startup time, shock loading/reduction of processing efficiency, uncontrolled detachment of sessile bacteria, and the ability to control microniche community formation for degradation of complex wastestreams. To improve bioreactor design in these areas, we have demonstrated a technique linking advanced cell immobilization to hollow fiber membrane bioreactor.

Porous silica immobilization of cells (biosilification) is a biocompatible, optically transparent encapsulation method used for high quality thin film deposition. Results indicate that encapsulated membrane-bound cells within biofilms are viable, retain their morphology, are metabolically active, and are physically trapped following biosilification. The resultant thin silica membrane is evenly distributed over the biofilm surface, reducing molecular diffusion limitations, and reinforcing the matrix. Both P. aeruginosa (a persistent chemoheterotroph) and N. europaea (a sensitive nitrogen cycling organism) survived the encapsulation process, and retained viability and physiology over an extended period of time (at least 30 days). The silica layer reduces the detachment of cells and polymers (improving biomass conversion rate), but does not constrict active detachment of cells (required for proper physiological biofilm self-maintenance). Planktonic cells are capable of forming a secondary layer of cells/polymers on silica-encapsulated biofilms, demonstrating.

The technique herein is scalable and capable of encapsulating complex geometries of immobilized bacteria by employing endogenous extracellular material as a site for silica deposition. These features will allow rapid deployment of bioreactors, which contain mature communities of microbes immobilized in biofilms, and will have the additional benefit of reducing uncontrolled biofilm erosion. Future and ongoing research will explore long term cellular viability, translation of the encapsulation system to new classes of cells, and “layering” of multispecies microbial communities in bioreactors for rapidly deployable processors for use in water reclamation systems.

Silica Entrapment of Biofilms in Membrane Bioreactors for Water Regeneration

Abstract

Habitat systems for long-term resource recovery must be reliable, safe and highly efficient, while providing potable water, oxygen, and edible biomass. Water makes up a large portion of the daily mass input into habitat systems. Considerations for water recycling technologies include shelf life, resupply-return logistics, maintenance time, power requirements, and footprint. Water recovery via physicochemical processes is limited by resupply, which can be alleviated by incorporation of an autonomous bioregenerative core, utilizing innate metabolic activity of cells to recover useable water from various wastestreams. Major components of bioregenerative core systems include plant/crop production systems and microbial bioreactors.

One of the microbial bioreactor technologies currently under consideration for use within closed loop water recovery systems is the membrane-aerated bioreactor (MABR). Although many advancements have been made regarding the optimization of MABR biotechnologies, problems that persist include: slow startup time, shock loading/reduction of processing efficiency, uncontrolled detachment of sessile bacteria, and the ability to control microniche community formation for degradation of complex wastestreams. To improve bioreactor design in these areas, we have demonstrated a technique linking advanced cell immobilization to hollow fiber membrane bioreactor.

Porous silica immobilization of cells (biosilification) is a biocompatible, optically transparent encapsulation method used for high quality thin film deposition. Results indicate that encapsulated membrane-bound cells within biofilms are viable, retain their morphology, are metabolically active, and are physically trapped following biosilification. The resultant thin silica membrane is evenly distributed over the biofilm surface, reducing molecular diffusion limitations, and reinforcing the matrix. Both *P. aeruginosa* (a persistent chemoheterotroph) and *N. europaea* (a sensitive nitrogen cycling organism) survived the encapsulation process, and retained viability and physiology over an extended period of time (at least 30 days). The silica layer reduces the detachment of cells and polymers (improving biomass conversion rate), but does not constrict active detachment of cells (required for proper physiological biofilm self-maintenance). Planktonic cells are capable of forming a secondary layer of cells/polymers on silica-encapsulated biofilms, demonstrating.

The technique herein is scalable and capable of encapsulating complex geometries of immobilized bacteria by employing endogenous extracellular material as a site for silica deposition. These features will allow rapid deployment of bioreactors, which contain mature communities of microbes immobilized in biofilms, and will have the additional benefit of reducing uncontrolled biofilm erosion. Future and ongoing research will explore long term cellular viability, translation of the encapsulation system to new classes of cells, and "layering" of multispecies microbial communities in bioreactors for rapidly deployable processors for use in water reclamation systems.

Introduction

Water is the most critical element for life support, and water regeneration is essential for establishing base camp self-sufficiency. Water recovery systems currently under development are intensive users of resources, including power for processes such as distillation and consumables for post treatment based on adsorption and chemical oxidation of contaminants. Alternative, low input systems are needed to maximize the logistics savings provided by water

recycling. Our proposed strategy for a more sustainable approach to water recycling relies on the integration of biological systems for regenerative oxidation of wastewater contaminants. Microbiological reactors are innately more regenerative than physiochemical systems. Adsorbents or catalysts with limited life spans are replaced by living cells that "recycle" the energy harnessed from oxidative reactions to carry out the reductive processes necessary for cell maintenance and growth.

There are a number of reactor types which have been investigated as bioprocessors in water recovery systems for life support applications, including biotrickling filters (McLamore et al., 2008), tubular reactors (Campbell et al., 1998), membrane aerated bioreactors (McLamore et al., 2007; Jackson et al., 2009; Chen et al., 2008), and various other biotechnologies based on immobilization of biofilms on engineered surfaces. A biofilm is defined as an agglomeration of microbial cell clusters enmeshed in an extracellular polymeric matrix (Costerson 2007).

In addition to stress response mechanisms globally expressed by suspended bacteria, microbes in biofilms form diverse communities capable of resisting large changes in influent composition (e.g., temperature, pH, nutrient loading rate, and chemical stressors). While there are many benefits to sessile growth, such as: increased resistance to antimicrobials (Stewart, 2002) and community-based defense mechanisms (Parsek and Greenberg, 2000), there are physiological costs associated with these advantages. EPS production imposes a metabolic burden, and intrabiofilm nutrient transport can limit growth and reduce the efficiency of stress response mechanisms (Huang et al., 1998; Hassett et al., 1999; Boles et al,. 2005).

A major source of bioreactor inefficiency is the detachment of active sessile cells from biofilms. Detachment can be caused by erosion, sloughing, abrasion, predator grazing, and active detachment. Erosion, sloughing, and abrasion are caused by fluid shear, and once the biofilm matures the mechanical removal of cells/polymers reaches a relatively constant rate (Characklis, 1990; Stoodley et al., 2001; Picioreanu et al., 2001). Active detachment is the dispersal of active cells from the biofilm matrix via physiological mechanisms triggered by environmental cues (Hunt et al., 2004; Sauer et al., 2004).

Uncontrolled biofilm detachment can cause many problems in engineered systems, including: an increase in the risk of human exposure to pathogenic bacteria, a reduction of hydrodynamic efficiency (bioclogging), process upset, and fouling of downstream processes. In water treatment/distribution systems, removal of biofilm can result in the detachment of inactivated (but potentially viable) microbes capable of reattachment and propagation (Stoodley et al., 2005). Proactive strategies for controlling biofilm formation in engineered systems include substratum surface modification (Veenendaal et al., 1999), limitation of free assimilable organic carbon, and turbulent bulk flow. Reactive strategies to control biofilms include: ultrasonication (Leriche and Carpentier, 1995), vortexing (Dhir and Dodd, 1995; Walker et al., 1993), addition of chemical disinfectant(s) (Robbins et al., 2005; Sule et al., 2007), cell signaling inhibition (Romeo, 2006), and starvation (Hunt et al., 2004). Although biofilm control strategies targeting EPS denaturation have been suggested (Simões et al. 2005**;** Ahimou et al., 2007), to date few techniques exist due to the complex dynamic phenomena occurring during detachment.

To alleviate many of the problems associated with sessile bacteria (e.g., uncrontrolled detachment, control of microniche community formation), we propose to develop modular, rapidly deployable biological systems by linking advanced cell immobilization techniques to the hollow fiber membrane bioreactors. Immobilization of the microorganisms on membranes will 1) provide stability to prevent erosion of the microorganisms into the effluent due to fluid shear; 2) support long-term survival and function of the microorganisms by providing a mechanically

stable polymeric matrix, 3) encourage metabolic state that optimizes bioreactor function, and 4) support the rapid start up of the bioreactor. To achieve these features, the microorganisms on hollow fiber membranes will be encapsulated by the deposition of porous silica using biosilicification techniques.

Cell-mediated silica entrapment

Silica based sol-gel glasses possess materials properties that make them appealing substrates for the encapsulation of pharmaceutical agents (Kortesuo, Ahola et al. 2000; Koehler, Zhao et al. 2008), enzymes (Bhatia, Brinker et al. 2000; Luckarift, Spain et al. 2004), and proteins (Ellerby, Nishida et al. 1992; Jedlicka, Little et al. 2007). The interconnected mesopourous amorphous glass network that forms due to the polycondensation of silicic acid molecules stabilizes sensitive biomolecules (Eggers and Valentine 2001), provides a large area for surface/solution interactions (Yang and Zhu 2005), and allows for the controlled release of entrapped agents (Roveri, Morpurgo et al. 2005). Sol-gels are typically synthesized using wet chemistry under ambient atmosphere at standard temperatures and pressures. This allows for the encapsulation of biological agents without denaturation or destruction (Avnir, Coradin et al. 2006). During the past two decades, researchers have expanded the scope of sol-gel technology to encapsulate living cells for a variety of applications (Avnir, Coradin et al. 2006; Prakash and Bhathena 2008). These include living biological sensors (Bottcher, Soltmann et al. 2004; Livage and Coradin 2006), catalysts (Carturan, Campostrini et al. 1989; Inama, Dire et al. 1993), and drug delivery devices (Bottcher, Soltmann et al. 2004; Avnir, Coradin et al. 2006; Coradin, Boissiere et al. 2006).

Many researchers employ variants of bulk gelation encapsulation techniques (Bottcher, Soltmann et al. 2004). Typically, cellular material is placed in an appropriate vessel and the liquid silica sol is introduced. This solution then gels to form a mesopourous silica glass that allows for the diffusion of nutrients and cellular products to and from the local environment. The resultant encapsulant is non-cell specific with material morphology governed by the surrounding vessel (Ferrer, Yuste et al. 2003; Nassif, Roux et al. 2003). The diffusional characteristics of such matrices are dependant on the thickness of the matrix and can vary widely from cell to cell (Satoh, Matsuyama et al. 1995; McCain and Harris 2003; Taylor, Finnie et al. 2004). While it is potentially possible to entrap large volumes of cells using these methods, diffusional constraints and the brittle nature of sol-gel glasses tend to preclude their use in large scale immobilization applications.

In order to address the limitations of current silica encapsulation technologies, we have developed a cell-specific biomimetic silfication technique inspired by stromatolytic bacterial formations. Cyanobacteria mats in silica rich hotsprings form ordered stromatilitic structures (Walter, Bauld et al. 1972). Observations in natural hotspring environments suggests that bacteria serve as sites for silica nucleation in a saturated environment (Konhauser and Ferris 1996; Konhauser, Phoenix et al. 2001; Mountain, Benning et al. 2003) with extracellular proteins and carbohydrates mediating the silification of the cells (Konhauser and Ferris 1996; Konhauser, Phoenix et al. 2001). The resultant amorphous silica layer allows for bacterial survival at depths of over 3mm (Konhauser and Ferris 1996; Konhauser, Phoenix et al. 2001).

We hypothesized that, given the chemical similarities between the organic matrix produced by cyanobacteria and other bacterial species, we could induce the formation of a cell or biofilm-specific mineralized layer by exposure to saturated silica solutions. Endogenous extracellular matrix molecules serve as a site for the preferential nucleation of a silica matrix.

Subsequent polycondensation of free silicic acid species then generates a mesopourous cell-specific membrane. Solution exchange or dilution then halts further deposition of silica, preventing bulk gelation.

To investigate the viability of our cell-mediated silica-based encapsulation technique, two model bacteria were grown in monoculture biofilms. *Pseudomonas aeruginosa* are commonly used in biomedical, and environmental applications (Xu, Stewart et al. 1998; Sauer, Camper et al. 2002), and thus were used as a model chemoheterotrophic bacteria. *Nitrosomonas europaea* are an important organism in biological nitrogen cycling in the environment, and were used as a model chemoautotrophic organism (Brandt, Hesselsoe et al. 2001; Coci, Riechmann et al. 2005). Mature biofilms were exposed to silifying solutions, and a battery of techniques used to (1) validate biomineralization by silica, (2) characterize viability, and (3) ensure physiological stress responses remained intact.

Methodology

Cell Culture

Pseudomonas aeruginosa is a chemohetertrophic gram negative opportunistic pathogen of animals, plants, and humans, and is used extensively as a model organism in wastewater treatment, bioremediation, and biomedical applications (Xu, Stewart et al. 1998; Ganguli and Tripathi 2002; Sauer, Camper et al. 2002; Vijayaraghavan and Yun 2008). *P. aeruginosa* (ATCC 97) was obtained from American Type Culture Collection (Manassas, VA), and biofilms were grown at 37°C in a glucose media (10mM glucose, 50mM HEPES, 3mM NH_4Cl, 43mM NaCl, 3.7mM KH_2PO_4, 1mM $MgSO_4$, and 3.5μM $FeSO_4$).

Nitrosomonas europaea is a chemoautotrophic gram negative bacteria that is often the rate limiting step in nitrogen cycling within the environment (Brandt, Hesselsoe et al. 2001; Coci, Riechmann et al. 2005). *N. europaea* are sensitive to changes in nutrient conditions, light, temperature, and chemical toxins, and thus are widely studied in soil, sewage, and freshwater systems. *N. europaea* (ATCC 19718) was obtained from ATCC, and biofilms were grown in ATCC medium 2265 (25.0 mM-$(NH_4)_2SO_4$, 43.0 mM-KH_2PO_4, 1.5 mM-$MgSO_4$, 0.25 mM-$CaCl_2$, 10 μM-$FeSO_4$, 0.83 μM-$CuSO_4$, 3.9 mM-NaH_2PO_4, and 3.74 mM-Na_2CO_3).

All cells were immobilized on semi-permeable silicon membranes in a hollow fiber membrane aerated bioreactor and grown under aerobic conditions according to McLamore et al. (McLamore, Jackson et al. 2007). Intact, mature immobilized biofilms will be extracted from the bioreactors via ¼" ferrules, and transferred to constructed flowcells prior to biosilification according to McLamore et al.(McLamore, Porterfield et al. 2009).

Enriched Silica Solution Preparation

Tetramethyl orthosilicate (TMOS, Sigma-Aldrich) was hydrolyzed in a 1:16 mol ratio (TMOS:H_20) deionized water solution using 1μl of 0.04 molar acid initiator (hydrochloric, nitric, or trifluoroacetic acid) per 1g of solution. The mixture was stirred vigorously for 10 minutes until clear. The methanol produced by the hydrolysis reaction was removed from the solution by rotary evaporation under vacuum at 45ºC (30% reduction in solution volume). The resulting saturated silica solution was refrigerated prior to use or used immediately.

Bulk liquid effluent measurements

Reactor efficiency was measured biweekly by collecting 10mL aliquots of effluent, and separating solutions for measurement of substrate, dissolved oxygen, and pH. NH_4^+ and pH

were measured using ThermoOrion ion-selective macroelectrodes, and dissolved oxygen was measured using a YSI meter (Yellow Springs International, Yellow Springs, OH). Glucose concentration was measured using a constructed biosensor (see following section) by continusouly stirring a 5mL at 200rpm.

Physiological Sensing

Glucose sensors were constructed using Pt/Ir microelectrodes (PI20033.0A10, 51mm length, 0.256mm shaft diameter, 1-2µm tip diameter, 3µm parylene-C coated metal shaft) obtained from Micro Probe Inc (Gaithersburg, MD). To construct the biosensor, Pt black was electro-deposited using a potentiostat (Applicable Electronics) in a solution of 0.72% chloroplatinic acid and 0.001% lead acetate. The microelectrode was connected to a cathode on the potentiostats, and a Pt wire 0.5mm in diameter (Alfa Aesar, Ward Hill, MA) was connected to the anode. A constant voltage (10V) was applied between the cathode and anode of the potentiostat for 1 minute. The MWNT solution was prepared by mixing 2mg MWNT in 1 ml Nafion, and ultrasonicating for 30 minutes. The MWNT solution (2µl) was cast on the tip of the microelectrode using a pipette, and the microelectrode was subsequently air dried for 5 minutes. For enzyme immobilization, the microelectrode was then dipped in 100 µl of a solution containing 50 mg-GOx/ml-PBS for 30 min.

Proton-selective microelectrodes were constructed following published procedures (Porterfield et al., 2009). Briefly, microelectrodes were fabricated for each experiment using non-filamented, 1.5 mm borosilicate glass capillaries (World Precision Instruments Inc., Sarasota, FL) pulled on a Sutter P-97 horizontal puller (Sutter instrument Co., Novato, CA), producing a tip diameter of 2-5 µm. Electrodes were then silanized using N-N dimethyl-trimethyl silane. The liquid ion exchange cocktail (proton cocktail A) was obtained from Fluka (St. Louis, MO), and the electrolyte contained 100mM KCl and 50mM HEPES buffer. Proton microelectrodes were calibrated using standard pH buffers (Sigma Aldrich, St. Louis, MO), and electromotive force was recorded at 1kHz against a Ag/AgCl reference electrode (3M KCl and 3% agar).

Fiber optic O_2 sensors (optrodes) used a frequency domain lifetime fluorometer and were constructed by pulling a 100/140 µm step index silica glass fiber cable on a Sutter P-2000 microprocessor controlled laser puller (Sutter instrument Co., Novato, CA), producing a tip diameter of 10 µm (Kühl and Jørgensen, 1992; Chatni and Porterfield, 2009). A polystyrene membrane containing platinum tetrakis (pentafluorophenyl) porphyrin (PtTFPP) was dip coated on the tip of the pulled fiber optic cable. The membrane contained 6.1% polystyrene (Sigma Aldrich, St. Louis, MO), 0.4% PtTFPP (Frontier Scientific, Logan, Utah), and 10.8% 2 µm diameter TiO2 microparticles (Sigma Aldrich, St. Louis, MO) dissolved in chloroform (Chatni and Porterfield, 2009; McLamore et al., 2010). Any temperature effects were corrected through the use of an integrated thermocouple that provided input for the digital signal processor-based lifetime fluorometer (Presence, Reganburg, Germany). Optrodes were calibrated in de-aerated, de-ionized (DI) water (nitrogen purged) and O2 saturated DI water (21%), and phase angle transduced to an analog signal via a digital signal processor (World Precision Instruments, Sarasota, FL).

To measure real time flux of metabolic analytes, a sensor technique known as self-referencing (SR) was used (Porterfield 2007). SR converts concentration sensors into dynamic biophysical flux sensors for quantifying real time transport in the cellular to whole tissue domain, and has been used in many fields, including: agricultural(Porterfield, Kuang et al. 1999;

Gilliham, Sullivan et al. 2006), biomedical (Land, Porterfield et al. 1999; Zuberi, Liu-Snyder et al. 2008), and environmental (Sanchez, Ochoa-Acuna et al. 2008) applications. SR discretely corrects for signals produced by ambient drift and noise by oscillating a microsensor between two locations at a fixed excursion distance according to Fick's first law of diffusion (Kuhtreiber and Jaffe 1990). The method quantifies real time changes in analyte concentration (ΔC) at two points separated by a known excursion distance (ΔX).

Non-invasive SR sensors were used to non-invasively quantify biofilm physiology using established methods (McLamore, Porterfield et al. 2009). A combination of electrochemical and optical sensors were employed to measure biochemical flux of oxygen and substrate for each monoculture biofilm. Briefly, oxygen flux was measured using a SR optical oxygen sensor, which was constructed by immobilizing an oxygen-quenched fluorescent dye (platinum tetrakis pentafluoropheynl porphyrin) on the tip of a tapered optical fiber. Change in phase angle was measured using a frequency-domain lifetime technique based on (30, Chatni and Porterfield, 2009). For *P. aeruginosa* biofilms, substrate (glucose) flux was amperometrically measured using a glucose biosensor which was fabricated by entrapping glucose oxidase within a Nafion/carbon nanotube layer on the tip of a platinized platinum wire according to (Shi et al., 2009). For *N. europaea*, substrate (NH_4^+) flux was measured using a microelectrode fabricated by immersing a Ag/AgCl wire in a tapered glass capillary containing electrolyte and a liquid membrane selective for NH_4^+ (Sauer et al., 2002).

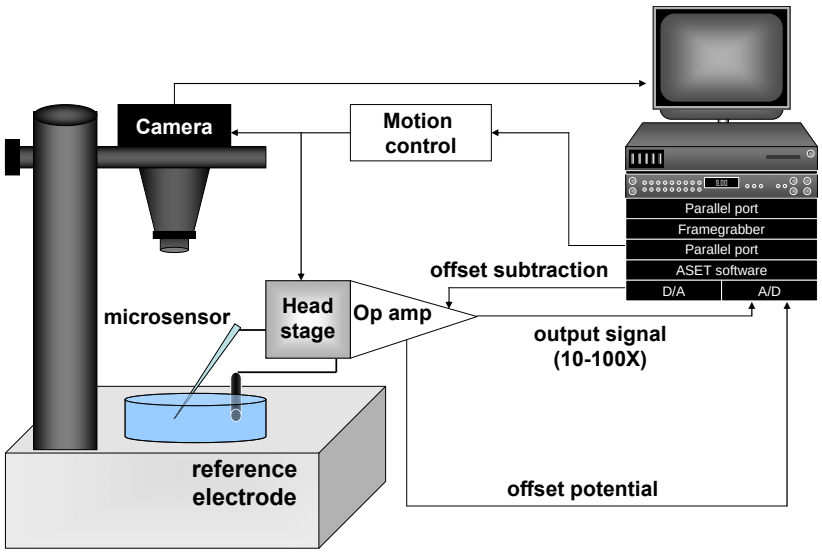

Figure 1. The self referencing sensor system is mounted on an anti-vibration table, and oscillation is conducted via remotely operated computer controlled stepper motors. Remote computer control contains frame grabber, computer with ASET software, D/A converter, and A/D converter.

For all experiments, substrate and/or O_2 flux were continuously measured at seven positions along the surface of each biofilm for ten minutes unless otherwise indicated (2mm in the lateral direction between each position; see supplemental Figure 1). For data concerning physiological flux, all averages represent the arithmetic mean of these 5 positions for (n=3) replicates, and error bars represent the standard error of the arithmetic mean.

Acid Initiator Screening

The three acid initiators were screened for biocompatibility with biofilms by continusouly measuring real time respiration using oxygen optrodes. Oxygen uptake was monitored for 10 minutes to determine baseline aerobic respiratory level. The media was carefully removed, and filtered media containing 10µl per ml enriched silica solution was carefully added, and allowed to rest 20 minutes in order to encapsulate the biofilm. Oxygen flux measurements were monitored throughout the biosilification process. After 20 minutes, the solution was again carefully removed and replaced with fresh silica free medium to halt the biosilification process. Oxygen flux measurements were then continuously recorded along the biofilm surface for 14 hours to monitor biofilm viability. As a control experiment, flux was measured in growth media, the solution was replaced with fresh growth media containing no silica, and physiological flux/viability measured.

SEM Imaging/Electron Dispersive X-ray (EDX) Elemental Analysis

P. aeruginosa and *N. europaea* biofilms were encapsulated with silica as described previously. Immediately after biofilm encapsulation, membranes containing immobilized, encapsulated biofilms were immersed in a 4% glutaraldehyde/sterile phosphate buffer solution for 1 hour. The samples were then soaked in deionized water for 15 minutes, followed by serial dehydration in ethanol solutions (25%, 50%, 75%, 90%, 100% respectively). Upon removal from the final ethanol wash, the samples were placed in a partially enclosed polystyrene dish and allowed to dry slowly under ambient conditions for 8 hours. Samples were then placed in a desiccating chamber prior to SEM imaging using a FEI NOVA nanoSEM high resolution FESEM.

For EDX analysis, coated biofilms were fixed in 4% glutaraldehyde/sterile phosphate buffer solution for 1 hour, washed four times in deionized water to remove residual media, and dried under ambient conditions for 8 hours. The samples were then placed in a desiccating chamber prior to analysis using an OXFORD INCA 250 electron dispersive X-ray detector (EDX). Spectra were collected over a 120x120µm area (n = 3). The spectral contribution of carbon was removed prior to analysis due to potential interference from the carbon tape fixative and the atomic percentage of the remaining elements (reported as %) was determined.

Confocal Imaging

Confocal microscopy was used to quantify membrane integrity after exposure to mineralizing solutions using a BacLight Live/Dead viability kit (Invitrogen Molecular Probes, Carlsbad, CA). The stain consistied of a nucleic acid (STYO9) and (propidium iodide) stain, and green and red stained cells represent cells with intact and damaged membranes, respectively. A Zeiss LSM 710 (Thornwood, NY) confocal microscope with multi-wavelength lasers (488 and 514nm) was used for excitation. Zen software (Zeiss, Thornwood, NY) was used for image capture. Nine cross sections of 144µm by 144µm were analyzed over a total biofilm depth of 128µm (2µm sections) using a 10X objective lens in immersion oil.

Bioenergetics

For uncoupling experiments, O_2 and H^+ flux were measured at seven positions along the biofilm surface for ten minutes (unless otherwise noted). While at the final position on the biofilm, real time O_2/H^+ flux were recorded during addition of 10µM carbonyl cyanide chlorophenyl hydrazone (CCCP). CCCP is an uncoupler of oxidative phosphorylation which

causes a temporary increase in O_2/H^+ flux as cells increase oxidative metabolism in an attempt to re-establish homeostasis (known as the "uncoupling" effect) (Spycher et al., 2008). During the time when the O_2/H^+ flux was in a heightened state (ca. 5-7 minutes), 10mM potassium cyanide (KCN) was added to abolish electron transport and ATP synthase activity (reducing proton and oxygen flux to minimal levels). Average values of O_2 and H^+ flux represent the mean of values recorded for at least 5 minutes.

Detachment

Detachment rate was quantified using particle counting via a coulter counter. After completion of *in situ* analysis of physiology and viability, all effluent and flow cell liquid was collected in autoclaved containers (approximately 7-8mL total sample volume). Detached particle size was quantified using a Beckman Multisizer 4 Coulter Counter (Beckman Coulter, Fullerton, CA). Samples were split in half, and one set of samples trypsinized for 16 minutes to digest suspended polymers as an internal control. Total particle count is a summation of polymeric material and cells/cell clusters. Trypsinization digests bioorganic suspended material by cleaving peptide chains at the carboxyl side of the amino acids. This leads to a reduction in size of polymeric material below detection limit (0.1μm), and also breaks up cell clusters. Thus, trypsinized data for these samples represents the total number of suspended cells, while untreated samples represents the number of bridged polymers (0.1-0.8μm) suspended cells (0.9-2μm), and cell clusters (2-10μm). Results from trypsizined samples were averaged and plotted along with average of untreated samples. Multiple aperture tubes (20 and 100μm) were utilized to quantify particle distribution in the 0.1-60μm range.

Results

Acid Initiator Screening

Respiratory oxygen flux for *P. aeruginosa* and *N. europaea* biofilms was not significantly different amongst control samples for all experiments ($p<0.01$, $\alpha=0.05$). Additionally, no significant difference was measured for control experiments (fresh growth media with no silica). Trifluoroacetic acid (TFA) significantly increased respiration rate in *P. aeruginosa* biofilms (285±14%), but had no significant effect on *N. europaea* respiration rate. This could be due to expression of stress response mechanisms expressed by *P. aeruginosa* which are not coded by *N. europaea* (e.g., efflux pumps, ion homeostatic regulation, netralizing enzymes/antioxidants) (Gilbert, McBain et al. 2002; Russell 2003). Conversely, hydrochloric acid (HCl) caused a significant increase in average respiratory rate for *N. europaea*, but had no significant effect on *P. aeruginosa*. For all samples using nitric acid as the initiator, no significant difference was measured between basal respiratory rate, control samples, and encapsulated biofilms. The bacteria respirome is extremely complex, and contains many stress response mechanisms associated with temperature stress, oxidative damage salt stress (Gilbert, McBain et al. 2002; Sauer, Camper et al. 2002; Coci, Riechmann et al. 2005), and many other changes in conditions. Thus, it is unclear as to the specific mechanism(s) behind these increased respiratory rates. Based on this screening technique, nitric acid was selected as the initiator, although initiation of silification with TFA and/or HCl should not be ruled out (McLamore et al., 2009[b]).

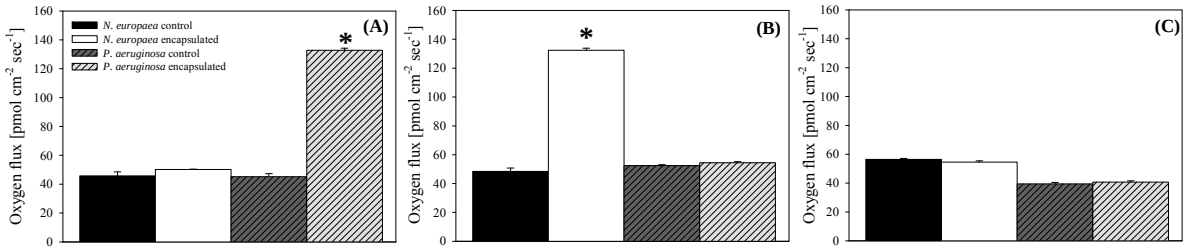

Figure 2. Average oxygen influx for *N. europaea* and *P. aeruginosa* biofilms before and five hours after cell-mediated encapsulation using (A) trifluoroacetic acid, (B) hydrochloric acid, and (C) nitric acid initiators. Asterik (*) indicates statistically significant difference between oxygen consumption for pre and post-encapsulation analyzed using ANOVA (n=3, α=0.05). Error bars represent ±2SE of the arithmetic mean at seven locations along the biofilm.

Verification of encapsulation

SEM images of biofilms taken 30 min after encapsulation exhibit morphological differences relative to controls. Cells encapsulated in silica retained a higher degree of structural fidelity (Fig 4. B), resisting the collapsing and smoothing effects of dehydration (Fig 4. A). In Fig 4. E, a silica matrix is bridging adjacent cells (indicated by a white arrow). Images taken of samples after 30 d of incubation do not display signs of a silica matrix and display feature collapse due to dehydration (Fig 4. C and F), which is indicative of the formation of new layers of cells on top of encapsulated cells.

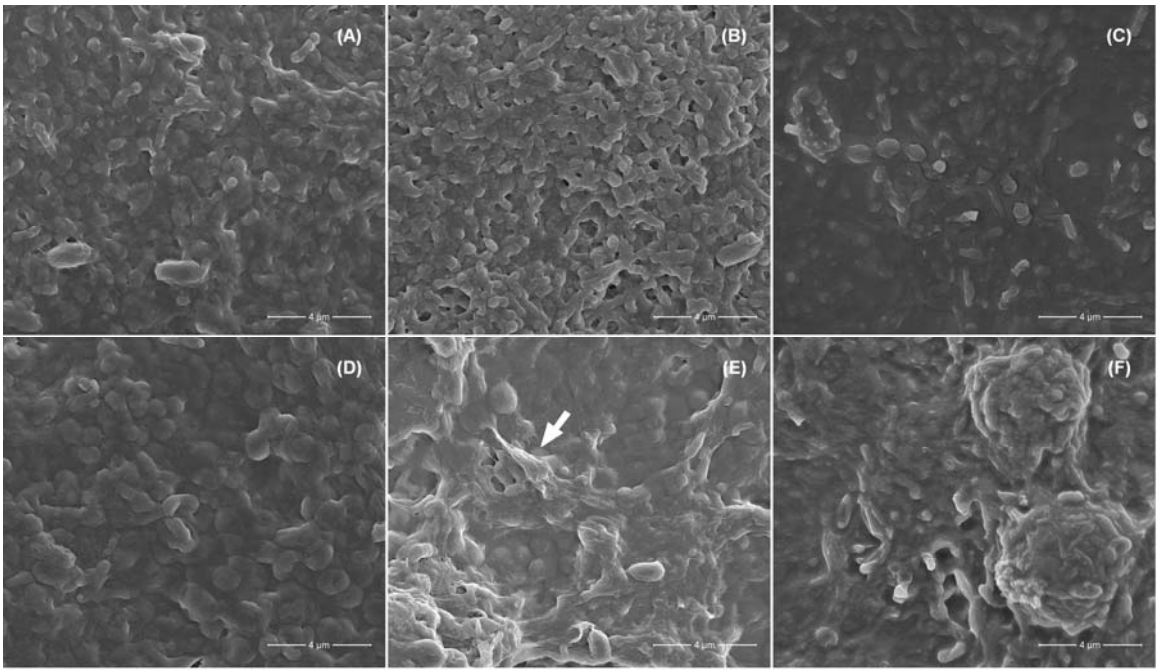

Figure 3. Representative electron microscopy images of *N europaea* biofilm (A) without silica deposition, (B) 30 minutes after encapsulation, and (C) 30 days after encapsulation. Images (D-F) represent unmodified *P. aeruginosa* biofilm, a biofilm encapsulated for 30 minutes, and a biofilm encapsulated for 30 days, respectively. The arrow illustrates silica matrix bridging cells. Scale bars represents 4µm.

Elemental analysis of the biofilm surfaces indicated that silica deposition took place after exposure to mineralizing solutions, causing an increase in silica concentration from 1.8±0.2 at% and 0.3±0.6 at% to 15.2±0.7 at% and 18.5±0.6 at% for *P. aeruginosa* and *N. europaea* respectively (Table 1). 30 days after encapsulation under constant operating conditions, the concentration of silica decreased to 2.0±0.5 at% and 1.0±0.1 at% for *P. aeruginosa* and *N. europaea*, respectively. Back scattered electron SEM imaging of *N. europaea* biofilms 30 days after encapsulation revealed several small areas with high contrast in elemental composition, and EDS revealed this was due to high levels of silica and aluminum 8.87 at% and 3.15 at%, respectively.

Table 1. Elemental composition (at%) of *P. aeruginosa* and *N. europaea* biofilms before biomineralization, 30min after encapsulation and 30d after encapsulation as determined by EDS spectral analysis.

P. aeruginosa	**O**	**Na**	**Al**	**Si**	**P**	**S**	**Cl**	**K**
Control	88.3±0.8	2.5±0.2	0	1.8±0.2	4.9±0.4	2.2±0.3	0	0.2±0.4
Si Coated 30min	76.7±1.0	1.4±0.5	0	15.2±0.7	2.0±0.4	0.8±0.2	3.5±1.4	0.4±0.1
Si Coated 30d	86.8±0.8	2.3±0.6	0.2±0.4	2.0±0.5	5.0±0.7	2.9±0.4	0.3±0.4	0.4±0.4
N. europaea								
Control	85.4±1.9	4.7±0.4	0	0.3±0.6	2.6±0.4	1.7±0.2	5.2±0.7	0
Si Coated 30min	75.5±0.9	1.3±0.3	0	18.5±0.6	1.2±0.1	1.0±0.1	2.5±0.3	0
Si Coated 30d	82.4±1.7	5.4±0.5	0	1.0±0.1	3.6±0.2	2.4±0.4	2.4±0.6	2.3±0.5

Viability and metabolic flux

Average bulk liquid (macroscale) substrate conversion rate (41±2%), dissolved oxygen concentration (52±5μM), and pH (6.9±0.4) measured in reactor effluent did not significantly change during 30 days of encapsulation for either species. These conversion rates are similar to previously published (McLamore et al., 2007). After the 30 day period, membrane-immobilized biofilms were extracted and transferred to flowcells for direct measurement of viability/physiology (microscale).

Average oxygen and substrate flux for *N. europaea* biofilms did not significant change following up to 30 days of encapsulation using TFA as an intiator. This is vital to the application of the biofilm silificaiton technique, as *N. europaea* has relatively few defense mechanisms and are sensitive to subtle changes in operating conditions (e.g., salt concentration, substrate shock) (Brandt, Hesselsoe et al. 2001; Coci, Riechmann et al. 2005). Likewise, metabolic respiratory rates for *P. aeruginosa* did not significantly change following 30 days of encapsulation using TFA. No significant differences in metabolic respiration were noted between silicated samples and control samples for either species.

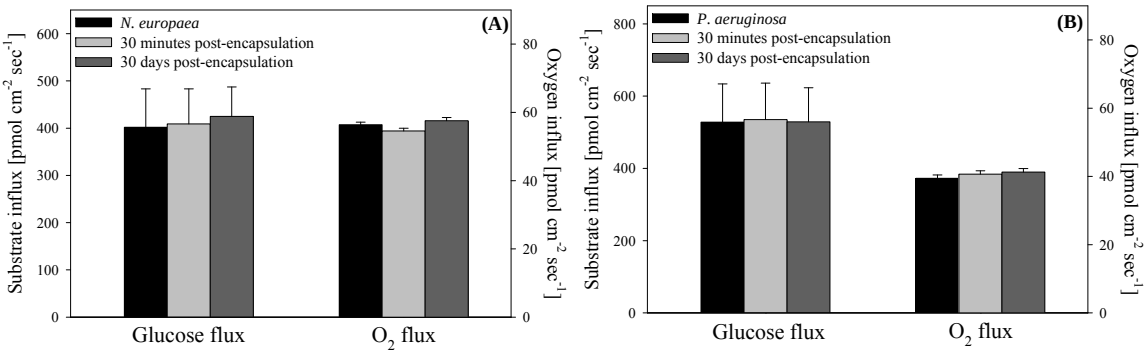

Figure 4. (A) Average oxygen and substrate influx for *N. europaea* biofilm before and after silica encapsulation. (B) Average oxygen and substrate flux for a *P. aeruginosa* biofilm before and after encapsulation. Average values represent 10 minutes of continuous recording at seven different positions along the biofilm surface. For all biofilms there was no significant spatial heterogeneity of flux ($p<0.01$, $\alpha=0.05$) along the surface (n=7 different positions separated by 1mm).

Viability was verified using a membrane integrity stain for all biofilm samples, and no significant difference was noted between control samples and silicated samples for up to 30 days. Representative images at 10X magnification are shown in Figure 3, and orthoganol views indicate no significant difference in profile and depth images. This was validated by cell counting at 100X magnification ($p=0.02$, $\alpha=0.05$).

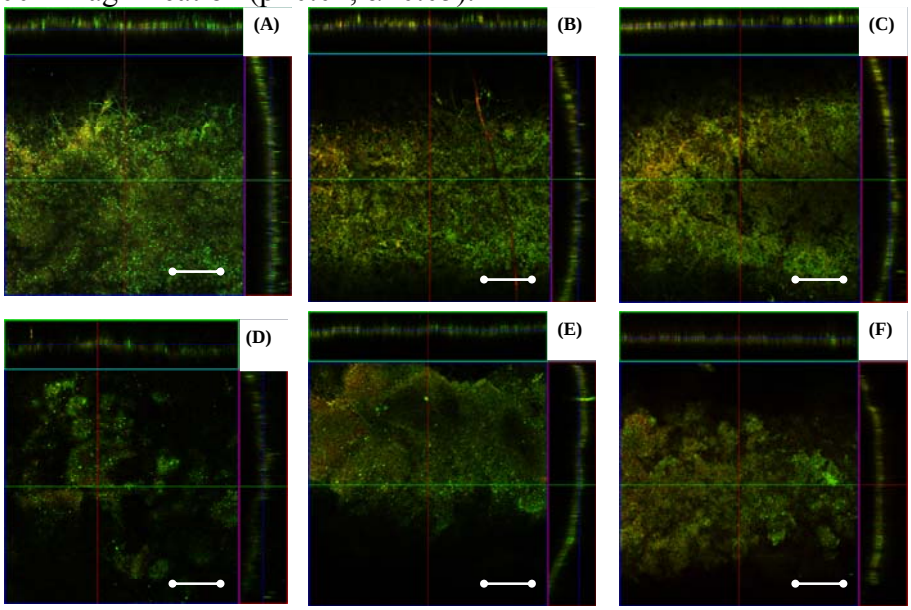

Figure 5. Representative confocal microscopy images (10X magnification) of *N europaea* biofilm (A) without silica deposition, (B) 30 minutes after encapsulation, and (C) 30 days after encapsulation. Images (D-F) represent an unmodified *P. aeruginosa* biofilm, a biofilm encapsulated for 30 minutes, and a biofilm encapsulated for 30 days, respectively. Biofilms were stained with a BacLight membrane integrity skit, where green represents cells with intact membranes, and red indicates cells which have lysed or damage membranes. No significant difference was observed following encapsulation for all samples, which was verified by cell counting with a 100X magnification. Scale bars represents 200µm. Orthoganol view represents composite of two dimensional images taken every 2µm over biofilm depth.

Bioenergetics and stress response

To verify that encapsulation did not affect cell physiology, a series of pharmacological experiments was conducted to analyze the bioenergetics of sessile cells within biofilms. In bacteria, oxygen, substrate, and proton flux mediate ATP production through a series of oxidative biochemical reactions (Figure 5). During aerobic respiration, oxygen influx drives ATP production via the tricaboxylic acid (TCA) cycle, glycolysis, and oxidative phosphorylation (OxPho). TCA and glycolysis contribute only a small fraction of total ATP production, and the majority of ATP production occurs via the OxPho system. Thus, most research characterizing bioenergetics targets the OxPho system. The electron transport complexes involved in OxPho (green structures in Figure 5) can be uncoupled from ATP synthase (red structure in Figure 5) by addition of pharmacological agents. The most common pharmacological experiment to study bioenergetics involves the addition of chemicals which "uncouple" electron transport from proton pumping and ATP production (Mitchell et al., 1961; Spycher et al., 2008).

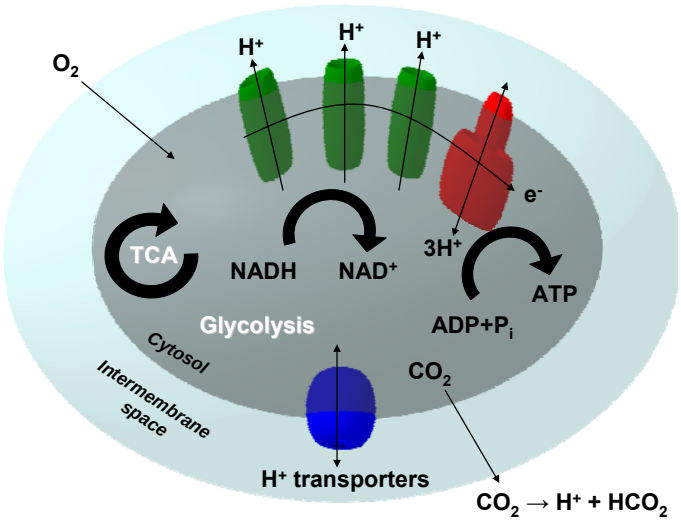

Figure 6. Bioenergetics of bacterial metabolism. Oxygen, substrate, and proton transport mediate production of ATP through a series of biochemical pathways (tricaboxylic acid cycling (TCA), glycolysis, and oxidative phosphorylation).

Continuous steady state O_2 influx and H^+ efflux was measured along the surface of control samples. A steady influx of O_2 drives aerobic respiration in *P. aeruginosa* and *N. europaea* cells. The direction of the proton flux in cells is not so intuitive. H^+ pumping from the cytosol across the intermembrane drives ATP production via proton motive force. However, the net movement of protons across cells depends on many factors, including the local concentration of buffers, metabolic state, rate of CO_2 production, and active stress response mechanisms (Spycher et al., 2008; McLamore et al., 2010). These complicating factors driving H^+ transport highlight the importance of using a phase-sensitive technique for characterizing physiology. In both species of biofilms, net proton efflux was measured along the surface of non-stressed biofilms (Figure 7). Following 30 minutes of continuous flux measurement (only five minutes are shown in Figure 5), cells were uncoupled using 20µM CCCP, causing a temporary increase of O_2 and H^+ flux which was maintained for at least three minutes in all samples. This increased O_2 and H^+ flux is a direct result of the uncoupling of electron transport form H^+ pumping by the OxPho system, and in preliminary experiments sessile cells were able to maintain this heightened

state of metabolic respiration for an average of 20 minutes after addition of CCCP. Subsequent addition of 10mM KCN abolished electron transport and reduced both O_2 and H^+ flux to insignificant levels within ten minutes for all samples.

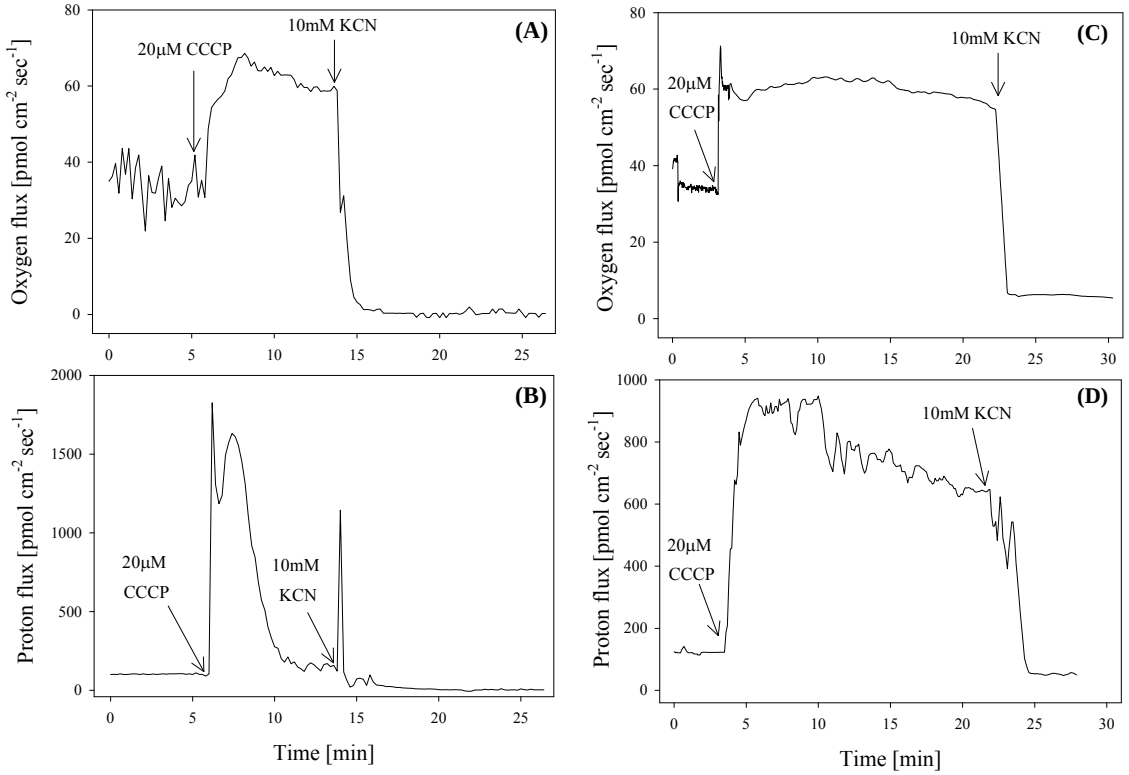

Figure 7. Uncoupling of oxidative phosphorylation in *N. europaea* biofilms showing real time (A) oxygen flux and (B) proton flux. *P. aeruginosa* uncoupling of (C) oxygen flux and (D) proton flux. Flux was recorded for 30 minutes prior to addition of CCCP (only five minutes shown), which uncoupled oxidative phosphorylation (causing an increase in oxygen and progon flux). After at least three minutes of steady state flux, 10mM KCN was added to abolish electron transport and reduce proton and oxygen flux.

These uncoupling experiments were repeated for biofilms which had been encapsulated for 30 days, and results indicated no significant difference compared to the response of control samples (Figure 8). In combination with the results regarding viability and substrate flux (Figures 3 and 4), these results clearly demonstrate that oxidative metabolism of cells was not affected by 30 days of encapsulation in silica.

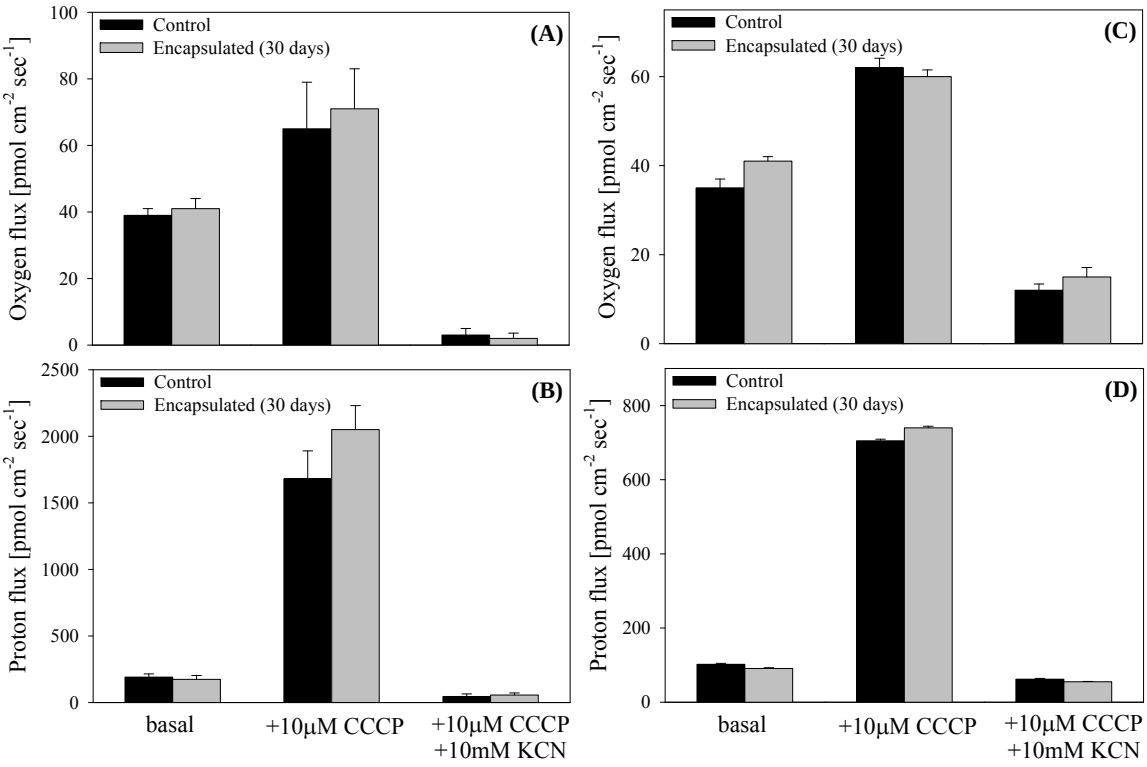

Figure 8. Uncoupling of oxidative phosphorylation in *N. europaea* biofilms showing average (A) oxygen flux and (B) proton flux for five replicate uncoated (conrol) and encapsulated (30 days) biofilm samples. Average (C) oxygen flux and (D) proton flux for five replicate control and encapsulated (30 days) *P. aeruginosa* biofilms. Average values represent at least three minutes of steady state flux, and error bars represent two times the standard error of the arithmetic mean. There was no significant difference between control samples and biofilms encapsulated for 30 days.

Detachment of sessile cells

Detachment of cells from biofilms was quantified before and after encapsulation under constant hydrodynamic conditions (Figure 7). For control samples, the average detachment rate normalized to fluid velocity (via Reynolds number) was $9.3X10^4$ for *N. europaea* biofilms $9.9X10^4$ for *P. aeruginosa* biofilms. This value was calculated by determining the slope of the curve in Figure 9A, and represents the average detachment rate within the fluid velocity operating range.

Approximately 30 minutes after silica deposition, net detachment rate was significantly reduced for both species by approximately 50±4%. For both species, the detachment rate following 30 days of encapsulation was an average of 24±7% lower than control samples, but significantly higher than samples encapsulated for 30days. This is due to the detachment of cells/polymers from the layer which formed on the surface of the silica layer (confirmed by electron microscopy, Figure 2).

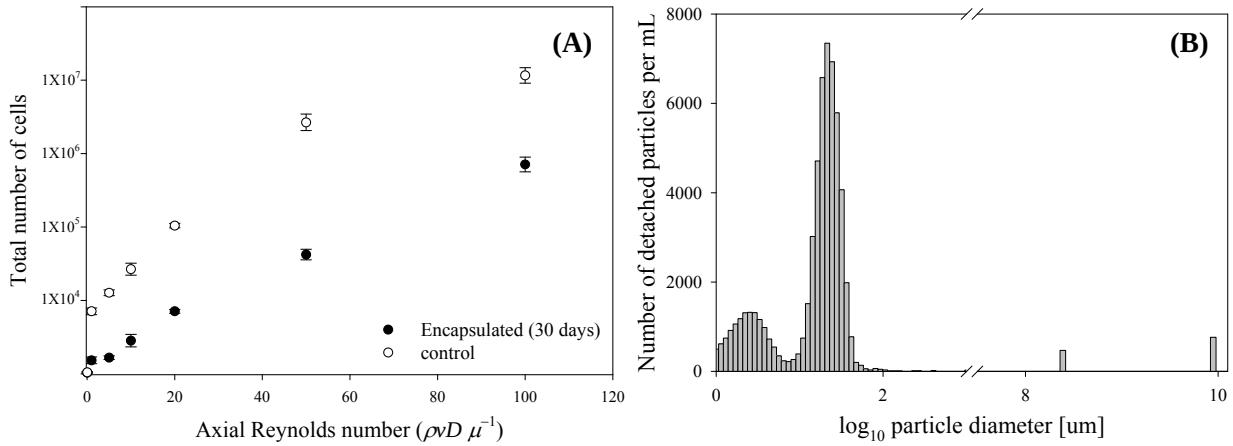

Figure 9. (A) Total number of detachment particles as a function of axial Reynolds number within the laminar regime (0-100). (B) Representative plot showing the ability to distinguish between detached polymers (0.1-0.5μm) and detached cells (0.9-2.0μm) based on particle size.

Discussion

The encapsulation system described in this study is analogous to that found in natural hot springs where silica leached from surrounding minerals saturates the aqueous environment (Hinman and Lindstrom 1996). When this solution comes into contact with bacterial mats (a dense, biofilm-like matrix), the extracellular polymeric matrix serves as a site for silica nucleation and polcondensation (SchultzeLam, Ferris et al. 1995; Phoenix, Adams et al. 2000). The current system involves artificially generating a saturated mineralizing environment through the use of organically modified silicates that hydrolyze in the presence of an acid initiator. Using the techniques herein, a metastable solution with silica concentrations in excess of what would be possible by heat assisted solubilization of silica mineral is obtained. In the laboratory these solutions are typically utilized to generate mesoporous silica sol-gel glasses (Brinker and Scherer 1990), where the high silica concentration allows formation of a solid hydrated matrix.

Proteins serve as a template for silica nucleation in organisms that form silica based structural elements such as sponges and diatoms (Kroger, Lorenz et al. 2002; Weaver and Morse 2003). The proteins of both sponges and diatoms share a certain degree of chemical similarity in that they are both enriched in hydroxyl amino acids such as tyrosine, threonine, and primarily serine (Hecky, Mopper et al. 1973; Shimizu, Cha et al. 1998; Sumper and Kroger 2004). These amino acids engage in ionic and hydrogen bonding interactions with -SiOH groups present in silicic acid containing solutions, generating sites for nucleation and polycondensation (Hecky, Mopper et al. 1973; Lobel, West et al. 1996; Kroger, Deutzmann et al. 1999). Alternatively, the hydroxyl groups may complex with phosphates to form preferential nucleation sites (Kroger, Lorenz et al. 2002). These same hydroxyl bearing groups are found distributed in the proteins of all organisms. While not evolved to form ordered structures, it was hypothesized that these endogenous proteins could serve as the site for silica deposition.

Given the random distribution of potential nucleation sites in biofilms (e.g., cell surface proteins and proteins in extracellular polymeric matrix), it was further hypothesized that the nanostructure of silica would resemble that of typical sol-gel glasses, as opposed to the condensed structures found in specialized organisms. The nanostructure of sol gels can be influenced by several factors including silica concentration, pH, curing temperature, and acid initiator species (Brinker and Scherer 1990). In the current study, we were constrained by the

necessity of maintaining organism viability, reducing the number of parameters that could be varied to influence nano-architecture. Temperature and final solution pH had to remain within the organism's optimal growth range, which is especially important for bacteria which are known to express a number of stress proteins related to temperature and pH shock (Gilbert, McBain et al. 2002; Russell 2003). In preliminary experiments, silica concentration was adjusted to provide a window where deposition occurred on the cellular substrate prior to bulk gelation. Given these constraints, three types of acid initiator (hydrochloric, nitric, and trifluoroacetic acid) were screened to determine their effects on biofilm viability. It was found that the respiration rate of cells encapsulated with silica hydrolyzed by a nitric acid did not significantly change, while hydrochloric and trifluoracetic acid significantly altered respiration ratewithin 30 minutes (Fig 1). Although the increases respiration rate observed in *P. aeruginosa* with triflouroacetic acid and *N. europaea* with hydrochloric acid are indicative of stress, further study is needed to determine the biochemical mechanisms associated with this stress response. However, based on our preliminary screening using aerobic respiratory rate, nitric acid initiated silica solutions were chosen for further investigation.

Using nitric acid as an initiator, SEM imaging and EDS elemental analysis confirmed the presence of a silica coating in both species of biofilm. SEM images of cells 30 min after coating demonstrated subtle differences in morphology (Fig 4, B and E) which were not observed in control samples or biofilms encapsulated for 30 days. These morphological differences were due to collapse of surface features in control and 30 day coated samples, while biofilms coated for 30 min were clearly delineated. This phenomenon is not surprising considering the increased stiffness expected from mineralized samples, and researchers have employed colloidal silica to improve preservation of biological samples for imaging. The apparent collapse in 30 d samples (Fig. 4, C and F) indicates the attachment and maturation of planktonic cells onto the silica layer formed during encapsulation. This result is expected, as both *P. aeruginosa* and *N. europaea* biofilms are known to grow on a wide variety of silica-based surfaces (Ghannoum and O'Toole 2004; Costerson 2007).

Encapsulated samples also demonstrated what appears to be a silica matrix connecting neighboring cells (Fig. 4, E arrow). EDS analysis confirmed the presence of this silica layer; samples analyzed 30 min after coating displayed a higher concentration of silica (18.49±0.59 and 15.24±0.67 at% for *N. europaea* and *P. aeruginosa,* respectively) than control samples (Table 1). After 30 d of incubation, the silica concentration present on the surface of the samples dropped to 1.02±0.07 and 2.03±0.45 at% for *N. europaea* and *P. aeruginosa* respectively. These silica concentrations are higher than control samples, but lower than samples coated for 30 minutes. The decrease in silica concentration in 30 d samples could arise from the dissolution of the silica layer or from the formation of a secondary biofilm on the encapsulated surface. Back scattered electron SEM imaging of the surface revealed variations in surface elemental cmpositions. Several small high-contrast areas were noted on the sample surface. EDS analysis of one of these areas demonstrated elevated silica and aluminum concentrations (8.87 and 3.15 at%, respectively). These findings suggest that a secondary biofilm covered most of the exposed encapsulated surface.

The presence of aluminum in conjunction with silica in the 30 d samples likely arises from silica's ability to fix aluminum ions in solution (Dugger, Stanton et al. 1964; Birchall 1995). This characteristic has been employed to remove metallic contaminants from wastewater (Zamzow, Eichbaum et al. 1990; Van Jaarsveld, Van Deventer et al. 1998). When utilized as an encapsulant for waste water treatment applications, silica's interaction with aluminum may

present a secondary health benefit. The incidence of Alzhimer's disease has been linked to elevated aluminum levels and lack of silica in the water supply (Rondeau, Jacqmin-Gadda et al. 2009).

No significant change in oxygen flux, substrate flux, or stoichiometric metabolism ratio was observed for up to 30 days after encapsulation ($p<0.02$, $\alpha= 0.05$). This was confirmed with a membrane integrity stain using confocal microscopy, and no significant difference was noted at 10X magnification or 100X magnification. There were no regions of lysed cells within the matrix (2μm slices), which one would expect if diffusion limitations or nutrient transport was significantly altered. Preservation of physiology and cell viability is particularly important for *N. europaea*, as encapsulation can potentially improve resistance to shock loading, chemical toxin exposure, and detachment.

To further validate that cells maintain proper physiological function when encapsulated, pharmacological experiments were conducted using the uncoupler CCCP and an inhibitor of electron transport (KCN). Steady O_2 and H^+ flux was not significantly different for control biofilms and biofilms encapsulated for 30 days. Both species of cells responded to uncoupling via CCCP addition, and subsequent respiratory inhibition by KCN. These experiments demonstrate that oxidative metabolism and stress response mechanisms of cells within biofilms were intact following biomineralization by silica. These oxidative stress response mechanisms are vital to the proper functioning of sessile cells, especially under dynamic substrate loading in applications such as wastewater treatment.

Encapsulation of biofilms significantly reduced the detachment rate, although cells and polymers which subsequently attached were prone to detachment. Due to the low cost and simplicity of the encapsulation method, these results suggest that the best technique for long term use may be a "layering" approach. There are engineering design opportunities to optimize the encapsulation process using this layering technique for both monoculture and mixed species biofilms. Improved control over community microniche formation in wastewater biofilms is a significant tehnological improvement, and will greatly improve the deployability of bioreactors for life support applications. However, encapsulation in an extremely thick silica layer is not optimal. In addition to leading to potential nutrient transport limitations, an excessively thick silica layer may limit active detachment of sessile cells. Active detachment (also known as seeding dispersal) is an important physiological regulator of biofilm thickness, and sessile cells continuously return to the planktonic state as a means of "spreading" (Purevdorj-Gage et al., 2005). This physiological mechanism must remain intact for proper function of the bioreactor, and thus the thickness fo the silica layer must be tightly controlled using such cell mediated encapsulation processes as the technique herein.

Conclusions

Safe, efficient water recovery systems are required for successful recycling of water and wastewater for human consumption/use. Microbial based technologies consume far less resources than physicochemical systems, and require less resupply of consumables. Thus, a bioregenerative core will be required for the optimum recovery of water/wastewater within life support/habitat systems. Although research has improved the operating efficiency of bioprocessors within water recovery systems, many problems still persist, including: slow startup time, inconsistent processing efficiency, and potential release of pathogens. The technique herein is designed to improve: (i) the rapid deployment of biofilm reactors, (ii) control over detachment of sessile bacteria from engineered surfaces within self-sufficient water regeneration

systems. To accomplish this, we demonstrate a technique linking advanced cell immobilization to the hollow fiber membrane bioreactors.

The technique is scalable and capable of encapsulating complex biofilm geometries by employing endogenous extracellular material as a site for silica deposition. As such, it can potentially be applied to a wide range of cell lines and mixed cellular systems. Both persistent *P. aeruginosa* and sensitive *N. europaea* species survive the encapsulation process, and retain viability and physiology over extended periods of time (at least 30 days). The silica layer is thin and evenly distributed over the cellular surface, reducing molecular diffusion limitations. The silica is also intimately associated with the extracellular proteins which reinforce the silica matrix and prevent cracking observed using bulk encapsulation methods. The silica layer reduces the detachment of cells and polymers (improving biomass conversion rate), but does not constrict active detachment of cells (required for proper physiological biofilm self-maintenance). The formation of a secondary layer of cells/polymers on silica-encapsulated biofilms is an important observation, and demonstrates that encapsulated cells are able to utilize detachment/reattachment processes necessary for proper function. These features will allow rapid deployment of bioreactors which contain mature communities of microbes immobilized in biofilms. Future and ongoing research will explore long term cellular viability, translation of the encapsulation system to new classes of cells, and "layering" of multispecies microbial communities in bioreactors for rapidly deployable processors for use in water reclamation systems.

References

Avnir, D., T. Coradin, et al. (2006). "Recent bio-applications of sol-gel materials." Journal of Materials Chemistry **16**(11): 1013-1030.

Bhatia, R. B., C. J. Brinker, et al. (2000). "Aqueous sol-gel process for protein encapsulation." Chemistry of Materials **12**(8): 2434-2441.

Birchall, J. D. (1995). "The Essentiality of Silicon in Biology." Chemical Society Reviews **24**(5): 351-&.

Bottcher, H., U. Soltmann, et al. (2004). "Biocers: ceramics with incorporated microorganisms for biocatalytic, biosorptive and functional materials development." Journal of Materials Chemistry **14**(14): 2176-2188.

Brandt, K. K., M. Hesselsoe, et al. (2001). "Toxic effects of linear alkylbenzene sulfonate on metabolic activity, growth rate, and microcolony formation of Nitrosomonas and Nitrosospira strains." Applied and Environmental Microbiology **67**(6): 2489-2498.

Brinker, C. J. and G. W. Scherer (1990). Sol-gel science.

Carturan, G., R. Campostrini, et al. (1989). "Inorganic Gels for Immobilization of Biocatalysts - Inclusion of Invertase-Active Whole Cells of Yeast (Saccharomyces-Cerevisiae) into Thin-Layers of Sio2 Gel Deposited on Glass Sheets." Journal of Molecular Catalysis **57**(1): L13-L16.

Chen, R.D., Semmens, M.J., LaPara, T.M. Biological treatment of a synthetic space mission wastewater using a membrane-aerated, membrane-coupled bioreactor (M2BR). Journal of Industrial Microbiology & Biotechnology, 2008, 35(6): 465-473.

Coci, M., D. Riechmann, et al. (2005). "Effect of salinity on temporal and spatial dynamics of ammonia-oxidising bacteria from intertidal freshwater sediment." Fems Microbiology Ecology **53**(3): 359-368.

Coradin, T., M. Boissiere, et al. (2006). "Sol-gel chemistry in medicinal science." Current Medicinal Chemistry **13**(1): 99-108.
Costerson, J. W., Ed. (2007). The Biofilm Primer. Berlin, Springer-Verlag.
Dugger, D. L., J. H. Stanton, et al. (1964). "Exchange of 20 Metal Ions with Weakly Acidic Silanol Group of Silica Gel." Journal of Physical Chemistry **68**(4): 757-&.
Eggers, D. K. and J. S. Valentine (2001). "Molecular confinement influences protein structure and enhances thermal protein stability." Protein Science **10**(2): 250-261.
Ellerby, L. M., C. R. Nishida, et al. (1992). "Encapsulation of Proteins in Transparent Porous Silicate-Glasses Prepared by the Sol-Gel Method." Science **255**(5048): 1113-1115.
Ferrer, M. L., L. Yuste, et al. (2003). "Biocompatible sol-gel route for encapsulation of living bacteria in organically modified silica matrixes." Chemistry of Materials **15**(19): 3614-3618.
Ganguli, A. and A. K. Tripathi (2002). "Bioremediation of toxic chromium from electroplating effluent by chromate-reducing Pseudomonas aeruginosa A2Chr in two bioreactors." Applied Microbiology and Biotechnology **58**(3): 416-420.
Ghannoum, M. and G. A. O'Toole, Eds. (2004). Microbial biofilms. Washingon, D.C., ASM Press.
Gilbert, P., A. J. McBain, et al. (2002). "Biocide abuse and antimicrobial resistance: being clear about the issues." Journal of Antimicrobial Chemotherapy **50**(1): 137-139.
Gilliham, M., W. Sullivan, et al. (2006). "Simultaneous flux and current measurement from single plant protoplasts reveals a strong link between K+ fluxes and current, but no link between Ca2+ fluxes and current." Plant Journal **46**(1): 134-144.
Hecky, R. E., K. Mopper, et al. (1973). "Amino-Acid and Sugar Composition of Diatom Cell-Walls." Marine Biology **19**(4): 323-331.
Hinman, N. W. and R. F. Lindstrom (1996). "Seasonal changes in silica deposition in hot spring systems." Chemical Geology **132**(1-4): 237-246.
Inama, L., S. Dire, et al. (1993). "Entrapment of Viable Microorganisms by Sio2 Sol-Gel Layers on Glass Surfaces - Trapping, Catalytic Performance and Immobilization Durability of Saccharomyces-Cerevisiae." Journal of Biotechnology **30**(2): 197-210.
Jackson, W.A., A. Morse, E.S. McLamore, T. Wiesner, and S. Xia (2009). "Nitrification-Denitrification Biological Pretreatment Systems for Potable Water Supply in Support of Space Exploration." Water Environment Research. 81(4) 423-431.
Jedlicka, S. S., K. M. Little, et al. (2007). "Peptide ormosils as cellular substrates." Journal of Materials Chemistry **17**(48): 5058-5067.
Koehler, J. J., J. Zhao, et al. (2008). "Compartmentalized Nanocomposite for Dynamic Nitric Oxide Release." Journal of Physical Chemistry B **112**(47): 15086-15093.
Konhauser, K. O. and F. G. Ferris (1996). "Diversity of iron and silica precipitation by microbial mats hydrothermal waters, Iceland: Implications for Precambrian iron formations." Geology **24**(4): 323-326.
Konhauser, K. O., V. R. Phoenix, et al. (2001). "Microbial-silica interactions in Icelandic hot spring sinter: possible analogues for some Precambrian siliceous stromatolites." Sedimentology **48**(2): 415-433.
Kortesuo, P., M. Ahola, et al. (2000). "Silica xerogel as an implantable carrier for controlled drug delivery - evaluation of drug distribution and tissue effects after implantation." Biomaterials **21**(2): 193-198.

Kroger, N., R. Deutzmann, et al. (1999). "Polycationic peptides from diatom biosilica that direct silica nanosphere formation." Science **286**(5442): 1129-1132.
Kroger, N., S. Lorenz, et al. (2002). "Self-assembly of highly phosphorylated silaffins and their function in biosilica morphogenesis." Science **298**(5593): 584-586.
Kuhtreiber, W. M. and L. F. Jaffe (1990). "Detection of extracellular calcium gradients with a calcium-specific vibrating electrode." J Cell Biol **110**(5): 1565-73.
Land, S. C., D. M. Porterfield, et al. (1999). "The self-referencing oxygen-selective microelectrode: Detection of transmembrane oxygen flux from single cells." Journal of Experimental Biology **202**(2): 211-218.
Livage, J. and T. Coradin (2006). Living cells in oxide glasses. Medical Mineraology and Geochemistry. Chantilly, Mineralogical Soc America. **64:** 315-332.
Lobel, K. D., J. K. West, et al. (1996). "Computational model for protein mediated biomineralization of the diatom frustule." Marine Biology **126**(3): 353-360.
Luckarift, H. R., J. C. Spain, et al. (2004). "Enzyme immobilization in a biomimetic silica support." Nature Biotechnology **22**(2): 211-213.
McCain, K. S. and J. M. Harris (2003). "Total internal reflection fluorescence-correlation spectroscopy study of molecular transport in thin sol-gel films." Analytical Chemistry **75**(14): 3616-3624.
McLamore, E., W. A. Jackson, et al. (2007). "Abiotic transport in a membrane aerated bioreactor." Journal of Membrane Science **298**(1-2): 110-116.
McLamore, E. S., D. M. Porterfield, et al. (2009). "Non-Invasive Self-Referencing Electrochemical Sensors for Quantifying Real-Time Biofilm Analyte Flux." Biotechnology and Bioengineering **102**(3): 791-799.
McLamore, E.S., D. Jaroch, J.L. Rickus, and D.M. Porterfield (2009). "Silica Entrapment of Biofilms in Bioreactors for Water Reuse in Life Support." Proceedings of the American Society for Gravitational and Space Biology.
Mitchell, P. Coupling of phosphorylation to electron and hydrogen transfer by a chemiosmotic type of mechanism. Nature. 1961, 191, 144–148.
Mountain, B. W., L. G. Benning, et al. (2003). "Experimental studies on New Zealand hot spring sinters: rates of growth and textural development." Canadian Journal of Earth Sciences **40**(11): 1643-1667.
Nassif, N., C. Roux, et al. (2003). "A sol-gel matrix to preserve the viability of encapsulated bacteria." Journal of Materials Chemistry **13**(2): 203-208.
O'Toole, G.A., Ghannoum, M. Microbial Biofilms, ASM Press, Washingon, D.C., 4-19.
Phoenix, V. R., D. G. Adams, et al. (2000). "Cyanobacterial viability during hydrothermal biomineralisation." Chemical Geology **169**(3-4): 329-338.
Porterfield, D. M. (2007). "Measuring metabolism and biophysical flux in the tissue, cellular and sub-cellular domains: Recent developments in self-referencing amperometry for physiological sensing." Biosensors & Bioelectronics **22**(7): 1186-1196.
Porterfield, D. M., A. X. Kuang, et al. (1999). "Oxygen-depleted zones inside reproductive structures of Brassicaceae: implications for oxygen control of seed development." Canadian Journal of Botany-Revue Canadienne De Botanique **77**(10): 1439-1446.
Prakash, S. and J. Bhathena (2008). "Live immobilised cells as new therapeutics." Journal of Drug Delivery Science and Technology **18**(1): 3-14.

Rondeau, V., H. Jacqmin-Gadda, et al. (2009). "Aluminum and Silica in Drinking Water and the Risk of Alzheimer's Disease or Cognitive Decline: Findings From 15-Year Follow-up of the PAQUID Cohort." American Journal of Epidemiology **169**(4): 489-496.

Roveri, N., M. Morpurgo, et al. (2005). "Silica xerogels as a delivery system for the controlled release of different molecular weight heparins." Analytical and Bioanalytical Chemistry **381**(3): 601-606.

Russell, A. D. (2003). "Similarities and differences in the responses of microorganisms to biocides." Journal of Antimicrobial Chemotherapy **52**(5): 750-763.

Sanchez, B. C., H. Ochoa-Acuna, et al. (2008). "Oxygen flux as an indicator of physiological stress in fathead minnow (Pimephales promelas) embryos: A real-time biomonitoring system of water quality." Environmental Science & Technology **42**(18): 7010-7017.

Satoh, S., I. Matsuyama, et al. (1995). "Diffusion of Gases in Porous Silica-Gel." Journal of Non-Crystalline Solids **190**(3): 206-211.

Sauer, K., A. K. Camper, et al. (2002). "Pseudomonas aeruginosa displays multiple phenotypes during development as a biofilm." Journal of Bacteriology **184**(4): 1140-1154.

SchultzeLam, S., F. G. Ferris, et al. (1995). "In situ silicification of an Icelandic hot spring microbial mat: Implications for microfossil formation." Canadian Journal of Earth Sciences **32**(12): 2021-2026.

Shi, J., A. Diggs, and D.M. Porterfield (2008). "A bionanocomposite glucose microbiosensor for biomedical and plant physiology applications." Proceedings of the Institute of Biological Engineers Annual Conference.

Shimizu, K., J. Cha, et al. (1998). "Silicatein alpha: Cathepsin L-like protein in sponge biosilica." Proceedings of the National Academy of Sciences of the United States of America **95**(11): 6234-6238.

Spycher, S.; Smejtek, P.; Netzeva T.I.; Escher B.I. Toward a Class-Independent Quantitative Structure-Activity Relationship Model for Uncouplers of Oxidative Phosphorylation. Chem. Res. Toxicol. 2008, 21, 911–927.

Sumper, M. and N. Kroger (2004). "Silica formation in diatoms: the function of long-chain polyamines and silaffins." Journal of Materials Chemistry **14**(14): 2059-2065.

Taylor, A. P., K. S. Finnie, et al. (2004). "Encapsulation of viable aerobic microorganisms in silica gels." Journal of Sol-Gel Science and Technology **32**(1-3): 223-228.

Van Jaarsveld, J. G. S., J. S. J. Van Deventer, et al. (1998). "Factors affecting the immobilization of metals in geopolymerized flyash." Metallurgical and Materials Transactions B-Process Metallurgy and Materials Processing Science **29**(1): 283-291.

Vijayaraghavan, K. and Y. S. Yun (2008). "Bacterial biosorbents and biosorption." Biotechnology Advances **26**(3): 266-291.

Walter, M. R., J. Bauld, et al. (1972). "Siliceous Algal and Bacterial Stromatolites in Hot Spring and Geyser Effluents of Yellowstone-National-Park." Science **178**(4059): 402-&.

Weaver, J. C. and D. E. Morse (2003). "Molecular biology of demosponge axial filaments and their roles in biosilicification." Microscopy Research and Technique **62**(4): 356-367.

Xu, K. D., P. S. Stewart, et al. (1998). "Spatial physiological heterogeneity in Pseudomonas aeruginosa biofilm is determined by oxygen availability." Applied and Environmental Microbiology **64**(10): 4035-4039.

Yang, H. P. and Y. F. Zhu (2005). "A high performance glucose biosensor enhanced via nanosized SiO2." Analytica Chimica Acta **554**(1-2): 92-97.

Zamzow, M. J., B. R. Eichbaum, et al. (1990). "Removal of Heavy-Metals and Other Cations from Waste-Water Using Zeolites." Separation Science and Technology **25**(13-15): 1555-1569.

Zuberi, M., P. Liu-Snyder, et al. (2008). Large naturally-produced electric currents and voltage traverse damaged mammalian spinal cord. **2:** 17.